

Alma Mater Studiorum Università di Bologna  
Archivio istituzionale della ricerca

Charge Separation and Recombination at Polymer-Fullerene Heterojunctions: Delocalization and Hybridization Effects

This is the final peer-reviewed author's accepted manuscript (postprint) of the following publication:

*Published Version:*

Davino, G., Muccioli, L., Olivier, Y., Beljonne, D. (2016). Charge Separation and Recombination at Polymer-Fullerene Heterojunctions: Delocalization and Hybridization Effects. THE JOURNAL OF PHYSICAL CHEMISTRY LETTERS, 7(3), 536-540 [10.1021/acs.jpcllett.5b02680].

*Availability:*

This version is available at: <https://hdl.handle.net/11585/576301> since: 2022-04-13

*Published:*

DOI: <http://doi.org/10.1021/acs.jpcllett.5b02680>

*Terms of use:*

Some rights reserved. The terms and conditions for the reuse of this version of the manuscript are specified in the publishing policy. For all terms of use and more information see the publisher's website.

This item was downloaded from IRIS Università di Bologna (<https://cris.unibo.it/>).  
When citing, please refer to the published version.

(Article begins on next page)

This is the final peer-reviewed accepted manuscript of:

**Charge Separation and Recombination at Polymer–Fullerene Heterojunctions:  
Delocalization and Hybridization Effects**

**Gabriele D’Avino, Luca Muccioli, Yoann Olivier, and David Beljonne**

***The Journal of Physical Chemistry Letters* 2016 7 (3), 536-540 .**

The final published version is available online at:  
<http://dx.doi.org/10.1021/acs.jpcllett.5b02680>

Rights / License:

The terms and conditions for the reuse of this version of the manuscript are specified in the publishing policy. For all terms of use and more information see the publisher's website.

*This item was downloaded from IRIS Università di Bologna (<https://cris.unibo.it/>)*

***When citing, please refer to the published version.***

This document is confidential and is proprietary to the American Chemical Society and its authors. Do not copy or disclose without written permission. If you have received this item in error, notify the sender and delete all copies.

### Charge Separation and Recombination at Polymer-Fullerene Heterojunctions: Delocalization and Hybridization Effects

Journal:	<i>The Journal of Physical Chemistry Letters</i>
Manuscript ID	jz-2015-026802.R1
Manuscript Type:	Letter
Date Submitted by the Author:	n/a
Complete List of Authors:	D'Avino, Gabriele; Université de Mons, Chimie des Matériaux Nouveaux Muccioli, Luca; University of Bordeaux, Laboratoire de Chimie des Polymères Organiques Olivier, Yoann; Université de Mons Beljonne, David; Université de Mons - UMONS / Materia Nova, Chimie des Matériaux Nouveaux & Centre d'Innovation et de Recherche en Matériaux Polymères; Université de Mons - UMONS / Materia Nova, Chimie des Matériaux Nouveaux & Centre d'Innovation et de Recherche en Matériaux Polymères

SCHOLARONE™  
Manuscripts

1  
2  
3  
4  
5  
6  
7  
8  
9  
10  
11  
12

# Charge separation and recombination at polymer- fullerene heterojunctions: Delocalization and hybridization effects

13  
14  
15  
16

*Gabriele D'Avino,<sup>†</sup> Luca Muccioli,<sup>§</sup> Yoann Olivier<sup>†</sup> David Beljonne<sup>†,\*</sup>*

17  
18

<sup>†</sup> Laboratory for Chemistry of Novel Materials, University of Mons, 7000 Mons, Belgium.

19  
20  
21  
22

<sup>§</sup> Laboratoire de Chimie des Polymères Organiques, UMR 5629, University of Bordeaux, 33607 Pessac, France.

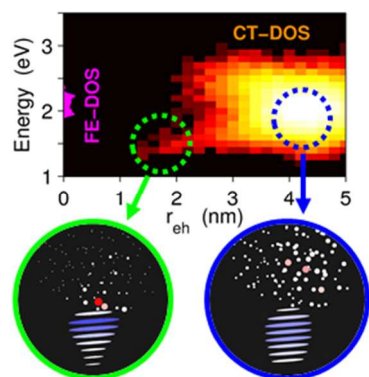
23  
24  
25  
26  
27  
28  
29  
30  
31  
32  
33  
34  
35  
36  
37  
38  
39  
40  
41  
42  
43  
44  
45  
46  
47  
48  
49  
50  
51  
52  
53  
54  
55  
56  
57  
58  
59  
60

\* David.Beljonne@umons.ac.be

## ABSTRACT

We address charge separation and recombination in polymer/fullerene solar cells with a multiscale modelling built from accurate atomistic inputs and accounting for disorder, interface electrostatics and genuine quantum effects on equal footings. Our results show that bound localized charge transfer states at the interface coexist with a large majority of thermally accessible delocalized space-separated states that can be also reached by direct photoexcitation, thanks to their strong hybridization with singlet polymer excitons. These findings reconcile the recent experimental reports of ultrafast exciton separation (“hot” process) with the evidence that high quantum yields do not require excess electronic or vibrational energy (“cold” process), and show that delocalization, by shifting the density of charge transfer states towards larger effective electron-hole radii, may reduce energy losses through charge recombination.

## TOC GRAPHICS



## KEYWORDS

organic photovoltaics, polymer-fullerene solar cells, multiscale modelling, exciton dissociation, charge recombination

1  
2  
3 Motivated by the prospects for high-efficiency organic solar cells, there have been considerable  
4 efforts to unveil the mechanisms of charge separation at donor/acceptor (D/A) heterojunctions.<sup>1,2</sup>  
5  
6 Though this is still a very much debated question, there is growing evidence that, in the best  
7  
8 devices, almost quantitative charge photogeneration from relaxed charge-transfer (CT) states  
9  
10 occurs without the need for excess electronic or vibrational energy,<sup>3-5</sup> possibly assisted by an  
11  
12 entropic gain ensured by the three-dimensional character of the fullerene acceptors.<sup>6,7</sup> This seems  
13  
14 to imply that exciton dissociation proceeds through weakly bound CT states, a mechanism  
15  
16 supported by microelectrostatic calculations of model interfaces.<sup>8-10</sup> On the other hand, a recent  
17  
18 report on charge separation occurring within a 40 fs time window over distances of a few nm in  
19  
20 fullerene-based bulk heterojunctions,<sup>11</sup> and other evidences of ultrafast phenomena,<sup>12-14</sup> point  
21  
22 instead to the combined role of delocalization effects and vibrationally-“hot” states in pulling  
23  
24 charges apart.<sup>15-17</sup> Yet, how do we reconcile these two nearly opposite pictures of charge  
25  
26 separation? And how do we account in the same framework for the massive recombination of  
27  
28 photogenerated charges, which has been identified as the main responsible for open-circuit  
29  
30 voltage losses<sup>18</sup> and that drastically limits the power conversion efficiency of organic solar cells?  
31  
32 To address these questions, we resort to a full atomistic theoretical description of charge pairs at  
33  
34 polymer-fullerene interfaces that accounts on an equal footing for electrostatic, disorder, and  
35  
36 delocalization effects. Our modelling reveals the presence of distinct populations of CT states  
37  
38 that are involved in the charge separation (CS) and charge recombination (CR) processes.  
39  
40 Namely, CS may occur both as a thermally activated process and by direct photoexcitation of  
41  
42 space-separated CT states acquiring oscillator strength due to strong mixing with resonant  
43  
44 polymer singlet excitons. We further show that CR, which originates from intermolecular  
45  
46  
47  
48  
49  
50  
51  
52  
53  
54  
55  
56  
57  
58  
59  
60

couplings among interfacial molecules, should be reduced by charge delocalization that shifts the density of CT states towards larger effective electron-hole (e-h) radii.

The description of the electronic structure at the length scale pertaining to charge separation at organic heterojunctions is a formidable task that we tackle with a multiscale approach grounded on a site-based model Hamiltonian fed with atomistic inputs. Our starting point is the realistic P3HT/PCBM interface in Figure 1a obtained from molecular dynamics simulations,<sup>9</sup> which defines molecular sites and their disordered connectivity. The electronic Hamiltonian is represented on a diabatic basis of localized states including the neutral state  $|0\rangle$ , singlet Frenkel excitons (FE)  $|i\rangle$ , and singlet-coupled CT states  $|i, j\rangle$  with  $i$  and  $j$  running on D and A sites, respectively. We consider explicitly the three low-lying unoccupied orbitals of fullerene derivatives,<sup>19</sup> so  $j$  is actually a composite index labelling A sites and orbitals. On this basis the Hamiltonian reads:

$$H = H_{CT} + H_{FE} + H_{CT-FE} \quad (1)$$

$$H_{CT} = \sum_{i,j} \varepsilon_{ij}^{CT} |i, j\rangle\langle i, j| + \sum_j \sum_{\langle i, i'\rangle} J_{ii'}^h |i, j\rangle\langle i', j| + \sum_i \sum_{\langle j, j'\rangle} J_{jj'}^e |i, j\rangle\langle i, j'| + \sum_{\langle i, j\rangle} J_{ij}^g |0\rangle\langle i, j| \quad (2)$$

$$H_{FE} = \sum_i \varepsilon_i^{FE} |i\rangle\langle i| + \sum_{\langle i, i'\rangle} J_{ii'}^x |i\rangle\langle i'|; H_{FE-CT} = \sum_{\langle i, j\rangle} J_{ij}^s |i\rangle\langle i, j| \quad (3)$$

Where  $H_{CT}$  accounts for the energy of electrostatically interacting CT states (diagonal energies  $\varepsilon_{ij}^{CT}$ ), for hole and electron transfer (CT couplings  $J_{ii'}^h$  and  $J_{jj'}^e$ ), and for ground-state charge transfer couplings ( $J_{ij}^g$ ) that are also responsible for CR.  $H_{FE}$  is the traditional Frenkel exciton model with site energies  $\varepsilon_i^{FE}$  and energy transfer couplings  $J_{ii'}^x$ , and finally  $H_{FE-CT}$  mixes Frenkel and CT excitons via the exciton splitting coupling  $J_{ij}^s$ .

1  
2  
3 Although similar models have been recently proposed,<sup>15,20–23</sup> the novelties over previous works  
4 are several, the most important being: (i) we move away from ideal lattices of reduced  
5 dimensionality in favor of the three-dimensional morphology of a realistic P3HT/PCBM  
6 interface; (ii) the CT states energies ( $\epsilon_{ij}^{CT}$ ) include the effect of electrostatic interactions with the  
7 polarizable environment as evaluated with classical microelectrostatic calculations;<sup>9,24</sup> (iii)  
8 electronic couplings driving charge and energy transfer are computed for molecular pairs  
9 extracted from the MD sample and hence explicitly account for structural disorder (see  
10 Experimental Section and SI). The proposed theoretical approach, bridging the gap between  
11 mesoscale electronic structure models and robust atomistic calculations, represents an important  
12 step towards a realistic description of the electronic states and processes at organic D/A  
13 interfaces.  
14  
15  
16  
17  
18  
19  
20  
21  
22  
23  
24  
25  
26  
27  
28  
29  
30  
31  
32  
33  
34  
35  
36  
37  
38  
39  
40  
41  
42  
43  
44  
45  
46  
47  
48  
49  
50  
51  
52  
53  
54  
55  
56  
57  
58  
59  
60

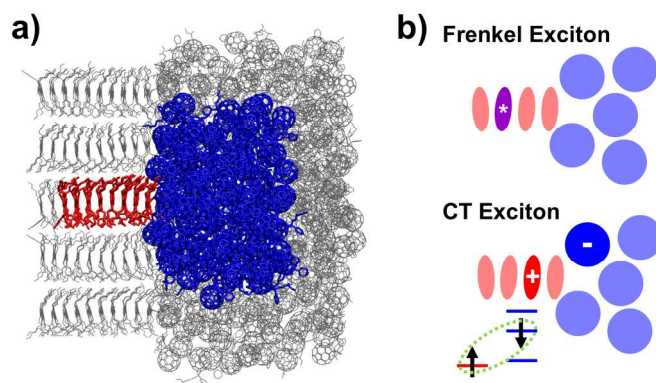


**Figure 1.** a) Snapshot of the P3HT/PCBM interface considered in this study; the colored region represents the subsystem described by Hamiltonian (1). b) Sketch of the molecular Frenkel exciton and singlet-coupled charge transfer states.



We start our discussion from *pure* CT states, i.e. the eigenstates of  $H_{CT}$  in Equation 2 that do not present any mixing with FEs. Our calculations confirm a very small CT in the ground state with less than 0.01 electrons of net charge on the D or A subsystem,<sup>21</sup> which corresponds to a negligible vacuum level shift (<5 meV) across the interface. The effect of charge delocalization on the energy landscape of CT states is addressed in Figure 2, where we compare the density of CT states (CT-DOS) computed according to three scenarios: (i) fully localized holes and electrons ( $J^h = J^e = 0$ ), (ii) delocalized electrons with localized holes ( $J^h = 0$ ), and (iii) fully delocalized holes and electrons. The average energy profile in the localized picture (Figure 2a) points to two populations of CT states: a low-energy tail of states with  $r_{eh} < 2$  nm that are electrostatically bound by 0.3-0.4 eV, and a dominant fraction of states featuring larger e-h radii and characterized by a rather flat energy profile.<sup>9</sup>

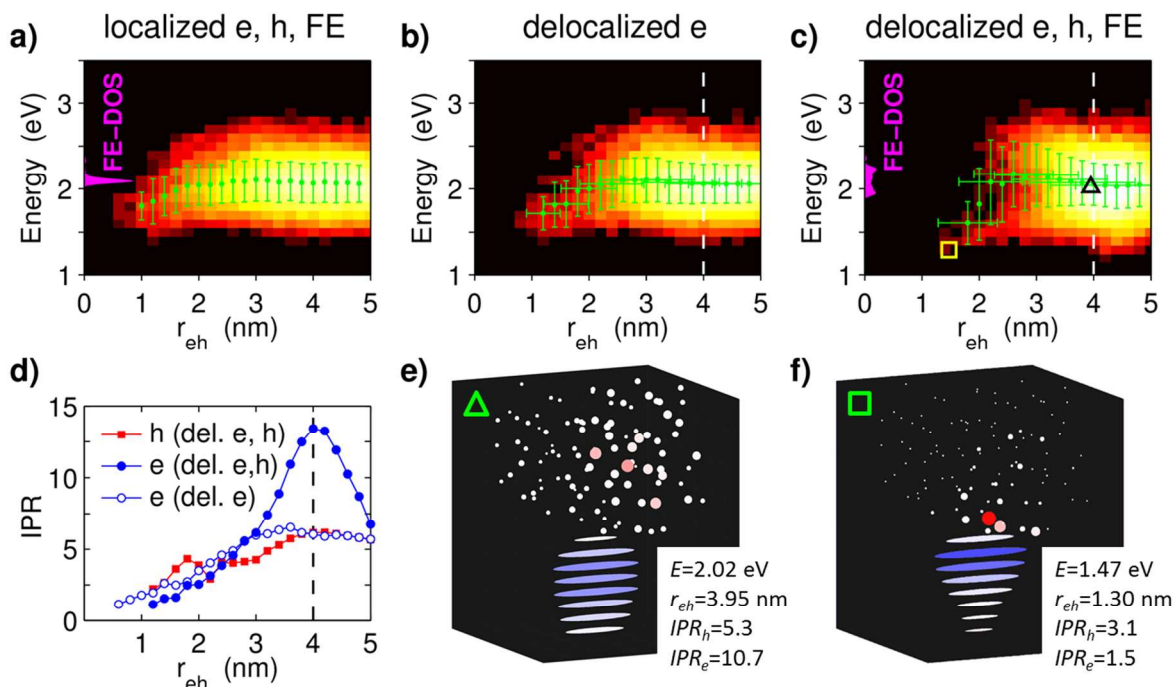


**Figure 2.** a-c) Density of pure CT states (heat map, logarithmic color scale) as a function of e-h distance and energy for localized and delocalized carriers. Green dots show the energy profile averaged in intervals of  $r_{eh}$ , vertical (horizontal) error bars report the standard deviation of energy (e-h mean spread) within each interval. Magenta areas in panel a) and c) show the DOS

1  
2  
3 of pure localized and delocalized FEs, respectively. d) Average inverse participation ratio (IPR)  
4 as a function of  $r_{eh}$ . e-f) Rendering of representative CT states, triangle and square recall panel c).  
5  
6  
7  
8  
9

10 The CT-DOS changes substantially when accounting for delocalization, especially when both  
11 electrons and holes can spread on multiple molecules. The remarkable difference between the  
12 CT-DOS in Figure 2b and 2c attests the importance of accounting for the delocalization of both  
13 carriers, at least for neat interfaces to large polymer crystallites. However, many  
14 polymer/fullerene blends present amorphous polymer domains and phase intermixing, hence we  
15 expect the actual scenario to be comprised between the pictures in Figure 2b and 2c.  
16  
17  
18  
19  
20  
21  
22  
23

24 Delocalization has a favorable effect on charge separation, as it stabilizes less Coulombically  
25 bound CT states at large e-h distance and shifts the CT-DOS to larger  $r_{eh}$ . Both charge carriers  
26 can in fact delocalize towards their respective transporting materials, leading to an increase of  
27 the average e-h distance, although many delocalized CT states have tails extending down to the  
28 interface. Charge delocalization, quantified by the inverse participation ratio (IPR, see Figure 2d),  
29 increases with  $r_{eh}$ , leading to CT states whose electronic clouds spread on average over ~13  
30 fullerenes at  $r_{eh} \sim 4$  nm, like the one rendered in Figure 2e. Nevertheless, a small population of  
31 more localized and bound CT states at small  $r_{eh}$  persists even when both electrons and holes are  
32 allowed to delocalize (square in Figure 2c and Figure 2f). This result is consistent with the  
33 distance distribution of (relaxed) photogenerated charges obtained by Barker *et al.*,<sup>25</sup> from the  
34 analysis of low-temperature recombination dynamics.  
35  
36  
37  
38  
39  
40  
41  
42  
43  
44  
45  
46  
47  
48  
49  
50

51 With a realistic description of the CT-DOS at hand, we can now turn our attention to FEs.

52 Because of the strong energy transfer couplings between P3HT decamers ( $J^x \approx 80$  meV), pure  
53 FEs ( $H_{FE-CT} = 0$ ) spread over the polymer stack leading to very different FE-DOS in the  
54  
55  
56  
57  
58  
59  
60

1  
2  
3 localized ( $J^x = 0$  in Equation 3, magenta area in Figure 2a) and delocalized picture (Figure 2c).  
4  
5  
6 The nature of the electronic excitations radically changes upon switching on the coupling with  
7  
8 CT states ( $H_{FE-CT}$ ), which leads to strong FE-CT *hybridization* as measured by their fractional  
9  
10 FE (CT) character  $v_{FE}$  ( $v_{CT}$ ). We quantify the number of excited states of nearly pure FE  
11  
12 character ( $v_{FE}>0.9$ ) to be only the 32% of that of (pure and localized) basis FEs. While these  
13  
14 numbers are specific to our model interface and system-size dependent, we point out that the  
15  
16 disappearance of pure FE in the close proximity of an interface is instead a general result, as also  
17  
18 suggested by many-body Bethe-Salpeter calculations on bimolecular complexes.<sup>26</sup> The weight of  
19  
20 FEs of interfacial polymer chains is therefore dispersed in the manifold of CT states, which, due  
21  
22 to their much larger number, maintain mostly  $v_{CT}\sim 1$ .  
23  
24  
25  
26  
27  
28

29 Strongly hybridized excitations should efficiently mediate the ultrafast conversion of pure FE  
30  
31 generated in the polymer bulk in high-energy CT states,<sup>27</sup> but also strongly affect the optical  
32  
33 properties of the D/A interface. Figure 3a shows the absorption cross section calculated for our  
34  
35 P3HT/PCBM interface, which resembles the P3HT H-aggregate absorption associated with FEs,  
36  
37 plus a weak low-energy tail due to the intrinsic CT absorption. The intense polymer absorption is  
38  
39 polarized along the backbone axis, while CT features have also an out-of-plane component. Even  
40  
41 though this is fully consistent with optical measurements,<sup>3</sup> our modelling further reveals that  
42  
43 much of the absorption intensity comes from states with a large CT character borrowing their  
44  
45 intensity from bright FEs: for our P3HT/PCBM interface the 62% of the integrated cross-section  
46  
47 is provided by states with  $v_{CT}>0.5$ . Moreover, most of this absorption corresponds to CT states  
48  
49 with an effective e-h distance larger than 3 nm and that are resonant with FE. This is better  
50  
51 shown by the  $r_{eh}$ -resolved absorption spectrum of hybrid CT states in Figure 3b, which reveals  
52  
53  
54  
55  
56  
57  
58  
59  
60

the correlation between absorption frequency and the effective distance between the photo-generated e-h pair.

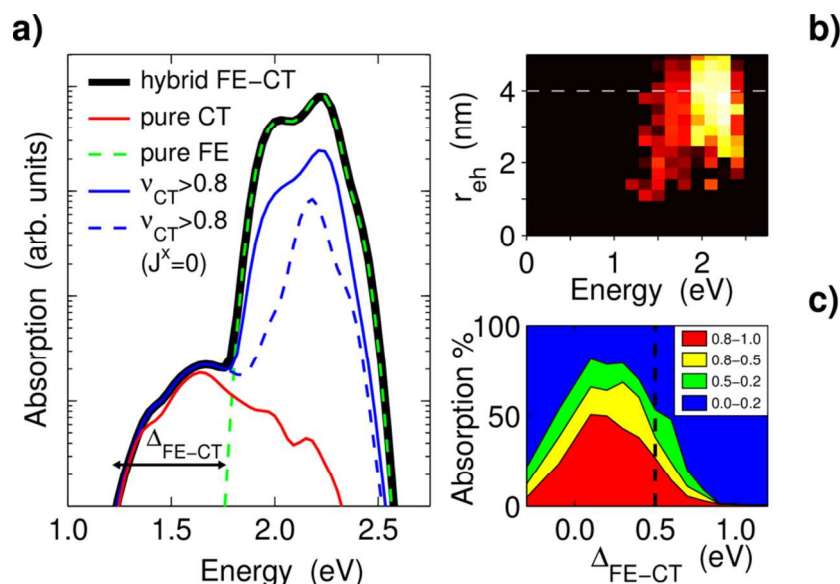


**Figure 3.** a) Absorption spectrum of the P3HT/PCBM interface computed with different models (see text). b) Absorption spectrum of hybrid CTEs resolved in energy and e-h distance, showing that most of CT transitions mainly yields space separated charges. c) Participation of states of different CT character ( $v_{CT}$  in the caption) to the total absorption cross-section as a function of  $\Delta_{FE-CT}$ . The vertical line at  $\Delta_{FE-CT}=0.5$  corresponds to P3HT/PCBM. For  $\Delta_{FE-CT}\sim 0.2$  half of the total absorption corresponds to states with  $v_{CT}>80\%$ .

This result confirms the possibility that primary photoexcitations in organic heterojunctions consist in space-separated CT states as suggested by Ma and Troisi for a model two-dimensional D/A interface.<sup>20</sup> The efficient optical generation of space-separated carriers requires delocalized CT states extending down to interface where these can mix with the FEs,<sup>20</sup> but also other material parameters play a key role. The offset between CT and FE absorptions, which can vary much in polymer/fullerene heterojunctions, is in fact also crucial for achieving large FE-CT mixing. Its effect is addressed in Figure 3c, where we show that the amount of absorption

1  
2  
3 intensity transferred to CT states is maximized for an optimal overlap between CT and FE DOSs.  
4  
5 The delocalization of FEs is also very important, as it mediates the coupling between CT states  
6  
7 and FEs of the inner polymer chains. Consequently, the absorption intensity of CT states is  
8  
9 expected to drop in systems featuring localized excitations, as illustrated in Figure 3a where we  
10  
11 compare the cross section of the excited states of prevailing CT character ( $v_{CT} > 0.8$ ) in the case of  
12  
13 delocalized (full blue line) and localized FEs ( $J^x = 0$ , blue dashed line).  
14  
15  
16  
17  
18  
19

20 We next address the critical aspect of charge recombination (CR), which is responsible for  
21  
22 voltage losses up to 0.7 eV in organic solar cells.<sup>18</sup> Despite several theoretical attempts to  
23  
24 compute CR rates,<sup>28-32</sup> the role of delocalization has been overlooked so far. Here, radiative and  
25  
26 nonradiative CR rates from all the excited states have been calculated in both cases of localized  
27  
28 and delocalized carriers. In the localized picture nonzero CR rates are found only for the few CT  
29  
30 states corresponding to D/A pairs in close contact at the interface, while sizeable rates are found  
31  
32 also for delocalized states with  $r_{eh} \geq 3$  nm. Following Burke *et al.*,<sup>18</sup> we assume thermal  
33  
34 equilibrium between Coulombically bound CT states and space-separated delocalized charges,  
35  
36 both described within our model, and compute Boltzmann averaged (non)radiative rates ( $\bar{k}_{NR}$ )  
37  
38  $\bar{k}_{RAD}$  that are given in Table 1. Our results are in overall accordance with experimental  
39  
40 values<sup>18,25</sup> and confirm that the nonradiative pathway is the dominant one. Delocalization is  
41  
42 found to reduce  $\bar{k}_{NR}$  by three orders of magnitude due to the dilution of interfacial localized CT  
43  
44 states into the dense manifold of low-energy space separated charges.  
45  
46  
47  
48  
49  
50  
51  
52  
53  
54

55 **Table 1.** Thermally averaged radiative and nonradiative CR rates in  $s^{-1}$  computed for the  
56 P3HT/PCBM interface for localized and delocalized carriers.  
57  
58  
59  
60

	Localized e and h	Delocalized e	Delocalized e and h
$\bar{k}_{RAD}$	$1.1 \cdot 10^6$	$5.9 \cdot 10^5$	$2.3 \cdot 10^5$
$\bar{k}_{NR}$	$3.0 \cdot 10^{10}$	$2.2 \cdot 10^{10}$	$4.8 \cdot 10^7$

Before concluding, we discuss to what extent our results for a specific and ideal P3HT/PCBM heterojunction can be generalized to polymer/fullerene solar cells, starting from the interface morphology. Fullerene typically forms disordered 3D clusters while soluble  $\pi$ -conjugated polymers aggregate in ordered lamellae or form amorphous and possibly intermixed regions characterized by loose electronic connectivity among polymer segments. Our model calculations, including the intermediate case of electron-only delocalization, capture these essential and general features of polymer-fullerene blends. Other general characteristics are the disordered intermolecular packing, and the reduction of the e-h separation energy barrier provided by the polarization of the microscopic environment, which are both missing in standard lattice models. Two key quantities that may be strongly system-dependent are the relative energies and couplings of FE and CT absorption features, which we vary in a broad range, and the electrostatic potential probed by charge carriers at the interface.

For our rather neat P3HT/PCBM interface the electrostatic potential is energetically favorable to e-h separation, substantially reducing the corresponding energy barrier by about 0.4 eV. This result depends, however, on several factors (i.e. materials chemical structure, interface morphology and macroscopic shape) and variations of similar magnitude, either favoring or disfavoring e-h separation energy-wise, have been computed<sup>32,33</sup> or measured<sup>34,35</sup> for other systems. Although the energy and distance distribution of CT states (and hence CR rates) depends on the details of the electrostatic landscape, the coexistence of bound localized CT

1  
2  
3 states and delocalized space-separated charges are general features we found also for the ideal  
4  
5 case of a uniform interfacial electrostatic landscape (see SI).  
6  
7

8 In summary, our modelling reveals the presence of states of different nature at organic D/A  
9  
10 heterojunctions, namely bound localized CT states at the interface and a large majority of  
11  
12 delocalized space-separated states; pure molecular FEs barely exist in the close proximity of the  
13  
14 interface and their absorption intensity is largely transferred to resonant CT states. This provides  
15  
16 a key for interpreting the early branching in the fate of photogenerated CT states observed for  
17  
18 several polymer/fullerene blends<sup>12,25</sup> and reconciles the observations of charge separation in the  
19  
20 ultra-fast and thermally activated regime, while showing that charge delocalization may slow  
21  
22 down charge recombination. The emerging picture confirms the crucial role of CT states and  
23  
24 their energetics that is largely governed by electrostatic interactions and morphology. High-  
25  
26 energy CT states, mostly superimposed to the polymer absorption, are pivotal for achieving high  
27  
28 charge yields, minimizing at the same time voltage losses.  
29  
30  
31  
32  
33  
34  
35  
36  
37

### 38 EXPERIMENTAL SECTION

39  
40 Parameters in Equations 1-3 are obtained from calculations performed on the structures of the  
41  
42 MD-simulated P3HT/PCBM interface in Ref. 9. FE energies and charge and energy transfer  
43  
44 couplings are evaluated at the semiempirical INDO/S level.  $\bar{k}_{NR}$  is computed with a Marcus-  
45  
46 Levich-Jortner formula suitably modified to account for delocalization,<sup>36</sup>  $\bar{k}_{RAD}$  is computed  
47  
48 assuming spontaneous emission. Results have been obtained for ten supramolecular clusters  
49  
50 similar to that in Figure 1a, sampling the whole interface of Ref. 9.  
51  
52  
53  
54  
55  
56  
57  
58  
59  
60

## ASSOCIATED CONTENT

**Supporting Information.** Comprehensive computational details. Distribution of charge and energy transfer couplings. Energetics of localized CT states. System size effects. Additional results. The following files are available free of charge.



## ACKNOWLEDGMENT

The work in Mons was supported by the Programme d'Excellence de la Région Wallonne (OPTI2MAT Project) and FNRS-FRFC. GD acknowledges support from EU through the FP7-PEOPLE-2013-IEF program (GA 2013-625198). D. B. is research director of FNRS. The work in Bordeaux has been funded by French National Grant ANR-10-LABX-0042-AMADEus managed by the National Research Agency under the initiative of excellence IdEx Bordeaux programme (Reference ANR-10-IDEX-0003-02).

## REFERENCES

- (1) Brédas, J.-L.; Norton, J. E.; Cornil, J.; Coropceanu, V. Molecular Understanding of Organic Solar Cells: The Challenges. *Acc. Chem. Res.* **2009**, *42* (11), 1691–1699.
- (2) Clarke, T. M.; Durrant, J. R. Charge Photogeneration in Organic Solar Cells. *Chem. Rev.* **2010**, *110* (11), 6736–6767.
- (3) Lee, J.; Vandewal, K.; Yost, S. R.; Bahlke, M. E.; Goris, L.; Baldo, M. A.; Manca, J. V.; Voorhis, T. Van. Charge Transfer State versus Hot Exciton Dissociation in Polymer-Fullerene Blended Solar Cells. *J. Am. Chem. Soc.* **2010**, *132* (34), 11878–11880.
- (4) Van Der Hofstad, T. G. J.; Nuzzo, D. Di; Van Den Berg, M.; Janssen, R. A. J.; Meskers, S. C. J. Influence of Photon Excess Energy on Charge Carrier Dynamics in a Polymer-Fullerene Solar Cell. *Adv. Energy Mater.* **2012**, *2* (9), 1095–1099.
- (5) Vandewal, K.; Albrecht, S.; Hoke, E. T.; Graham, K. R.; Widmer, J.; Douglas, J. D.; Schubert, M.; Mateker, W. R.; Bloking, J. T.; Burkhard, G. F.; et al. Efficient Charge Generation by Relaxed Charge-Transfer States at Organic Interfaces. *Nat. Mater.* **2014**, *13* (1), 63–68.
- (6) Gregg, B. A. Entropy of Charge Separation in Organic Photovoltaic Cells: The Benefit of Higher Dimensionality. *J. Phys. Chem. Lett.* **2011**, *2* (24), 3013–3015.
- (7) Monahan, N. R.; Williams, K. W.; Kumar, B.; Nuckolls, C.; Zhu, X.-Y. Direct Observation of Entropy-Driven Electron-Hole Pair Separation at an Organic Semiconductor Interface. *Phys. Rev. Lett.* **2015**, *114* (24), 247003.
- (8) Verlaak, S.; Beljonne, D.; Cheyns, D.; Rolin, C.; Linares, M.; Castet, F.; Cornil, J.; Heremans, P. Electronic Structure and Geminate Pair Energetics at Organic–Organic Interfaces: The Case of Pentacene/C60 Heterojunctions. *Adv. Funct. Mater.* **2009**, *19* (23), 3809–3814.
- (9) D'Avino, G.; Mothy, S.; Muccioli, L.; Zannoni, C.; Wang, L.; Cornil, J.; Beljonne, D.; Castet, F. Energetics of Electron–Hole Separation at P3HT/PCBM Heterojunctions. *J. Phys. Chem. C* **2013**, *117* (25), 12981–12990.
- (10) Castet, F.; D'Avino, G.; Muccioli, L.; Cornil, J.; Beljonne, D. Charge Separation Energetics at Organic Heterojunctions: On the Role of Structural and Electrostatic Disorder. *Phys. Chem. Chem. Phys.* **2014**, *16* (38), 20279–20290.

- 1  
2  
3  
4  
5  
6  
7  
8  
9  
10  
11  
12  
13  
14  
15  
16  
17  
18  
19  
20  
21  
22  
23  
24  
25  
26  
27  
28  
29  
30  
31  
32  
33  
34  
35  
36  
37  
38  
39  
40  
41  
42  
43  
44  
45  
46  
47  
48  
49  
50  
51  
52  
53  
54  
55  
56  
57  
58  
59  
60
- (11) Gelinas, S.; Rao, A.; Kumar, A.; Smith, S. L.; Chin, A. W.; Clark, J.; van der Poll, T. S.; Bazan, G. C.; Friend, R. H. Ultrafast Long-Range Charge Separation in Organic Semiconductor Photovoltaic Diodes. *Science (80-. )*. **2013**, *343*, 512.
- (12) Bakulin, a. a.; Rao, a.; Pavelyev, V. G.; van Loosdrecht, P. H. M.; Pshenichnikov, M. S.; Niedzialek, D.; Cornil, J.; Beljonne, D.; Friend, R. H. The Role of Driving Energy and Delocalized States for Charge Separation in Organic Semiconductors. *Science (80-. )*. **2012**, *335* (6074), 1340–1344.
- (13) Jailaubekov, A. E.; Willard, A. P.; Tritsch, J. R.; Chan, W.-L.; Sai, N.; Gearba, R.; Kaake, L. G.; Williams, K. J.; Leung, K.; Rossky, P. J.; et al. Hot Charge-Transfer Excitons Set the Time Limit for Charge Separation at Donor/acceptor Interfaces in Organic Photovoltaics. *Nat. Mater.* **2013**, *12* (1), 66–73.
- (14) Grancini, G.; Maiuri, M.; Fazzi, D.; Petrozza, A.; Egelhaaf, H.-J.; Brida, D.; Cerullo, G.; Lanzani, G. Hot Exciton Dissociation in Polymer Solar Cells. *Nat. Mater.* **2013**, *12* (1), 29–33.
- (15) Tamura, H.; Burghardt, I. Ultrafast Charge Separation in Organic Photovoltaics Enhanced by Charge Delocalization and Vibronically Hot Exciton Dissociation. *J. Am. Chem. Soc.* **2013**, *135* (44), 16364–16367.
- (16) Huix-Rotllant, M.; Tamura, H.; Burghardt, I. Concurrent Effects of Delocalization and Internal Conversion Tune Charge Separation at Regioregular Polythiophene–Fullerene Heterojunctions. *J. Phys. Chem. Lett.* **2015**, 1702–1708.
- (17) Falke, S. M.; Rozzi, C. A.; Brida, D.; Maiuri, M.; Amato, M.; Sommer, E.; De Sio, A.; Rubio, A.; Cerullo, G.; Molinari, E.; et al. Coherent Ultrafast Charge Transfer in an Organic Photovoltaic Blend. *Science* **2014**, *344* (6187), 1001–1005.
- (18) Burke, T. M.; Sweetnam, S.; Vandewal, K.; McGehee, M. D. Beyond Langevin Recombination: How Equilibrium Between Free Carriers and Charge Transfer States Determines the Open-Circuit Voltage of Organic Solar Cells. *Adv. Energy Mater.* **2015**, *5* (11), 201500123.
- (19) D’Avino, G.; Olivier, Y.; Muccioli, L.; Beljonne, D. Do Charges Delocalize over Multiple Molecules in Fullerene Derivatives? *J. Mater. Chem. C* **2016**.
- (20) Ma, H.; Troisi, A. Direct Optical Generation of Long-Range Charge-Transfer States in Organic Photovoltaics. *Adv. Mater.* **2014**, *26*, 6163–6167.
- (21) Raos, G.; Casalegno, M.; Idé, J. An Effective Two-Orbital Quantum Chemical Model for Organic Photovoltaic Materials. *J. Chem. Theory Comput.* **2013**, *10*, 364–372.
- (22) Savoie, B. M.; Rao, A.; Bakulin, A. a.; Gelinas, S.; Movaghar, B.; Friend, R. H.; Marks, T. J.; Ratner, M. a. Unequal Partnership: Asymmetric Roles of Polymeric Donor and Fullerene Acceptor in Generating Free Charge. *J. Am. Chem. Soc.* **2014**, *136* (7), 2876–2884.
- (23) Bittner, E. R.; Silva, C. Noise-Induced Quantum Coherence Drives Photo-Carrier Generation Dynamics at Polymeric Semiconductor Heterojunctions. *Nat. Commun.* **2014**, *5*, 3119.
- (24) D’Avino, G.; Muccioli, L.; Zannoni, C.; Beljonne, D.; Soos, Z. G. Electronic Polarization in Organic Crystals: A Comparative Study of Induced Dipoles and Intramolecular Charge

- 1  
2  
3 Redistribution Schemes. *J. Chem. Theory Comput.* **2014**, *10* (11), 4959–4971.
- 4  
5 (25) Barker, A. J.; Chen, K.; Hodgkiss, J. M. Distance Distributions of Photogenerated Charge  
6 Pairs in Organic Photovoltaic Cells. *J. Am. Chem. Soc.* **2014**, *136*, 12018.
- 7  
8 (26) Duchemin, I.; Blase, X. Resonant Hot Charge-Transfer Excitations in Fullerene-Porphyrin  
9 Complexes: Many-Body Bethe-Salpeter Study. *Phys. Rev. B* **2013**, *87* (24), 245412.
- 10  
11 (27) Chen, K.; Barker, A. J.; Reish, M. E.; Gordon, K. C.; Hodgkiss, J. M. Broadband Ultrafast  
12 Photoluminescence Spectroscopy Resolves Charge Photogeneration via Delocalized Hot  
13 Excitons in Polymer:fullerene Photovoltaic Blends. *J. Am. Chem. Soc.* **2013**, *135* (49),  
14 18502–18512.
- 15  
16 (28) Lemaur, V.; Steel, M.; Beljonne, D.; Brédas, J. L.; Cornil, J. Photoinduced Charge  
17 Generation and Recombination Dynamics in Model Donor/acceptor Pairs for Organic  
18 Solar Cell Applications: A Full Quantum-Chemical Treatment. *J. Am. Chem. Soc.* **2005**,  
19 *127* (16), 6077–6086.
- 20  
21 (29) Yi, Y.; Coropceanu, V.; Brédas, J.-L. Exciton-Dissociation and Charge-Recombination  
22 Processes in pentacene/C60 Solar Cells: Theoretical Insight into the Impact of Interface  
23 Geometry. *J. Am. Chem. Soc.* **2009**, *131* (43), 15777–15783.
- 24  
25 (30) Liu, T.; Troisi, A. Absolute Rate of Charge Separation and Recombination in a Molecular  
26 Model of the P3HT/PCBM Interface. *J. Phys. Chem. C* **2011**, *115* (5), 2406–2415.
- 27  
28 (31) Liu, T.; Cheung, D. L.; Troisi, A. Structural Variability and Dynamics of the  
29 P3HT/PCBM Interface and Its Effects on the Electronic Structure and the Charge-Transfer  
30 Rates in Solar Cells. *Phys. Chem. Chem. Phys.* **2011**, *13* (48), 21461.
- 31  
32 (32) Idé, J.; Méreau, R.; Ducasse, L.; Castet, F.; Bock, H.; Olivier, Y.; Cornil, J.; Beljonne, D.;  
33 D'Avino, G.; Roscioni, O. M.; et al. Charge Dissociation at Interfaces between Discotic  
34 Liquid Crystals: The Surprising Role of Column Mismatch. *J. Am. Chem. Soc.* **2014**, *136*  
35 (7), 2911–2920.
- 36  
37 (33) Poelking, C.; Andrienko, D. Design Rules for Organic Donor-Acceptor Heterojunctions:  
38 Pathway for Charge Splitting and Detrapping. *J. Am. Chem. Soc.* **2015**, 150422153017001.
- 39  
40 (34) Burke, T. M.; McGehee, M. D. How High Local Charge Carrier Mobility and an Energy  
41 Cascade in a Three-Phase Bulk Heterojunction Enable 90% Quantum Efficiency. *Adv.*  
42 *Mater.* **2014**, *26* (12), 1923–1928.
- 43  
44 (35) Sweetnam, S.; Graham, K. R.; Ndjawa, G. O. N.; Heumu, T.; Bartelt, J. A.; Burke, T. M.;  
45 Li, W.; You, W.; Amassian, A.; McGehee, M. D. Characterization of the Polymer Energy  
46 Landscape in Polymer:Fullerene Bulk Heterojunctions with Pure and Mixed Phases. **2014**,  
47 No. Cv.
- 48  
49 (36) Caruso, D.; Troisi, A. Long-Range Exciton Dissociation in Organic Solar Cells. *Proc.*  
50 *Natl. Acad. Sci.* **2012**, *109* (34), 13498–13502.
- 51  
52  
53  
54  
55  
56  
57  
58  
59  
60